AMERICAN JOURNAL OF PHYSICAL ANTHROPOLOGY 106:87–100 (1998)

Patterns of Strain in the Macaque Ulna During Functional Activity

BRIGITTE DEMES,[1,3,*] JACK T. STERN, JR.,[1,3]
MICHAEL R. HAUSMAN,[2] SUSAN G. LARSON,[1,3]
KENNETH J. MCLEOD,[3] AND CLINTON T. RUBIN[1,3]
[1]*Department of Anatomical Sciences, School of Medicine, State University of New York, Stony Brook, New York 11794-8081*
[2]*Department of Orthopedics, Mount Sinai School of Medicine, New York, New York 10029*
[3]*Program in Biomedical Engineering, Health Sciences Center, State University of New York, Stony Brook, New York 11794-8181*

ABSTRACT In vivo bone strain experiments were performed on the ulnae of three female rhesus macaques to test how the bone deforms during locomotion. The null hypothesis was that, in an animal moving its limbs predominantly in sagittal planes, the ulna experiences anteroposterior bending. Three rosette strain gauges were attached around the circumference of the bone slightly distal to midshaft. They permit a complete characterization of the ulna's loading environment. Strains were recorded during walking and galloping activities. Principal strains and strain directions relative to the long axis of the bone were calculated for each gauge site. In all three animals, the lateral cortex experienced higher tensile than compressive principal strains during the stance phase of walking. Compressive strains predominated at the medial cortex of two animals (the gauge on this cortex of the third animal did not function). The posterior cortex was subject to lower strains; the nature of the strain was highly dependent on precise gauge position. The greater principal strains were aligned closely with the long axis of the bone in two animals, whereas they deviated up to 45° from the long axis in the third animal.

A gait change from walk to gallop was recorded for one animal. It was not accompanied by an incremental change in strain magnitudes. Strains are at the low end of the range of strain magnitudes recorded for walking gaits of nonprimate mammals.

The measured distribution of strains in the rhesus monkey ulna indicates that mediolateral bending, rather than anteroposterior bending, is the predominant loading regime, with the neutral axis of bending running from anterior and slightly medial to posterior and slightly lateral. A variable degree of torsion was superimposed over this bending regime. Ulnar mediolateral bending is apparently caused by a ground reaction force vector that passes medial to the forearm. The macaque ulna is not reinforced in the plane of bending. The lack of buttressing in the loaded plane and the somewhat counterintuitive bending direction recommend caution with regard to conventional interpretations of long bone cross-sectional geometry. Am J Phys Anthropol 106:87–100, 1998.

KEY WORDS in vivo bone strain; macaque ulna; functional morphology

Inherent to functional interpretations of shapes of bones are assumptions about their mechanical behavior and the forces and moments to which they are exposed. It is

Contract grant sponsor: National Science Foundation; Contract grant number: SBR 9507078.

*Correspondence to: Brigitte Demes, Department of Anatomical Sciences, State University of New York, Stony Brook, NY 11794-8081. E-mail: bdemes@mail.som.sunysb.edu.

Received 15 July 1997; accepted 31 January 1998.

common practice to model long bones as beams loaded by muscle, joint, and substrate reaction forces. The external forces and moments are extrapolated from observations of limb action during postural and locomotor activities. Ideally, quantified limb kinematics and experimentally determined substrate reaction forces and muscle activity are used to predict the loading patterns. Even then, the situation is complicated by the irregular shapes of long bones, which deviate from the simple geometric beam analogues. Consequently, actual loadings can be deduced only with a certain degree of plausibility. Does limb action in sagittal planes translate into bending in this plane (see, e.g., Ruff and Runestad, 1992; Demes and Jungers, 1993)? Does the greater versatility of movements that is said to characterize primates imply a greater range of loading patterns of their limb bones and, consequently, the need for more robust bones (Kimura, 1995; Polk et al., 1997)? The assumptions inherent in the models can be tested only by measuring the deformations of bones directly during various activities.

The numbers of in vivo studies of long bone deformation are limited and are restricted to mostly cursorial, nonprimate mammals (Lanyon and Smith, 1969, 1970; Lanyon and Baggott, 1976; Goodship et al., 1979; Lanyon and Bourn, 1979; Lanyon et al., 1979; Carter et al., 1981; Rubin and Lanyon, 1982, 1984; Biewener et al., 1983, 1988; Bouvier and Hylander, 1984; Biewener and Taylor, 1986; Gross et al., 1992; Swartz et al., 1992; Biewener and Bertram, 1993). In one of these studies, Biewener et al. (1983) demonstrated discrepancies between loading patterns reconstructed from the orientation of the ground reaction force vector and limb posture and those determined from in vivo bone strain recordings for the horse metacarpus, substantiating the suspicion that loading reconstructions may lead to spurious results.

In vivo bone strain data for primate postcranial bones exist for the proximal ulna of a spider monkey (Fleagle et al., 1981), the forelimb bones of gibbons (Swartz et al., 1989), and the tibia of humans (Lanyon et al., 1975; Burr et al., 1996). Macaques were chosen for our project to add the first strictly quadrupedal primate to the data base. The three primate species for which strain data have been recorded so far rely exclusively, or to a significant extent, on only one pair of limbs for locomotion, which makes it difficult to compare them directly with the nonprimate quadrupeds for which strain data are available. Various kinematic and kinetic aspects of quadrupedal locomotion differ between primates and nonprimate mammals. Primates have been shown to walk with longer strides, greater angular excursions, and lower stride frequencies (Alexander and Maloiy, 1984; Reynolds, 1987; Demes et al., 1994). They tend to carry more weight on their hind limbs (Kimura et al., 1979; Demes et al., 1994). Primates also have relatively longer limbs than nonprimate mammals (Alexander et al., 1979). It remains to be seen whether primate quadrupeds differ from nonprimate quadrupeds in bone strain levels or in any other aspect of the strain environment.

To completely characterize the loading regime of a long bone, information from three, three-element gauges attached to the bone at the same transverse plane is required (Gross et al., 1992). Gauge implantation should be accomplished without cutting through muscles, and gauge sites should be distant enough from muscle attachment sites to avoid local stress concentrations unrelated to the global deformation of the bone. Only a few long bones lend themselves to such an analysis. We have chosen to study strain in the ulna. Based on limb action primarily in the sagittal plane coupled with an active tripeps muscle during the stance phase of locomotion, we hypothesized that the ulna experiences anteroposterior bending with the posterior surface in tension and the with the anterior surface in compression.

The ulna and the elbow display significant variation among primates that correlates with locomotor modes (see, e.g., Fleagle et al., 1975; Fleagle, 1983; Rose, 1988; Harrison, 1989; Richmond et al., in press). The elbow joint of terrestrial mammals is characterized by lateral and medial flanges at the margins of the trochlea that supposedly act to stabilize the joint (Jenkins, 1973). Cercopithecoids display this morphology, with a

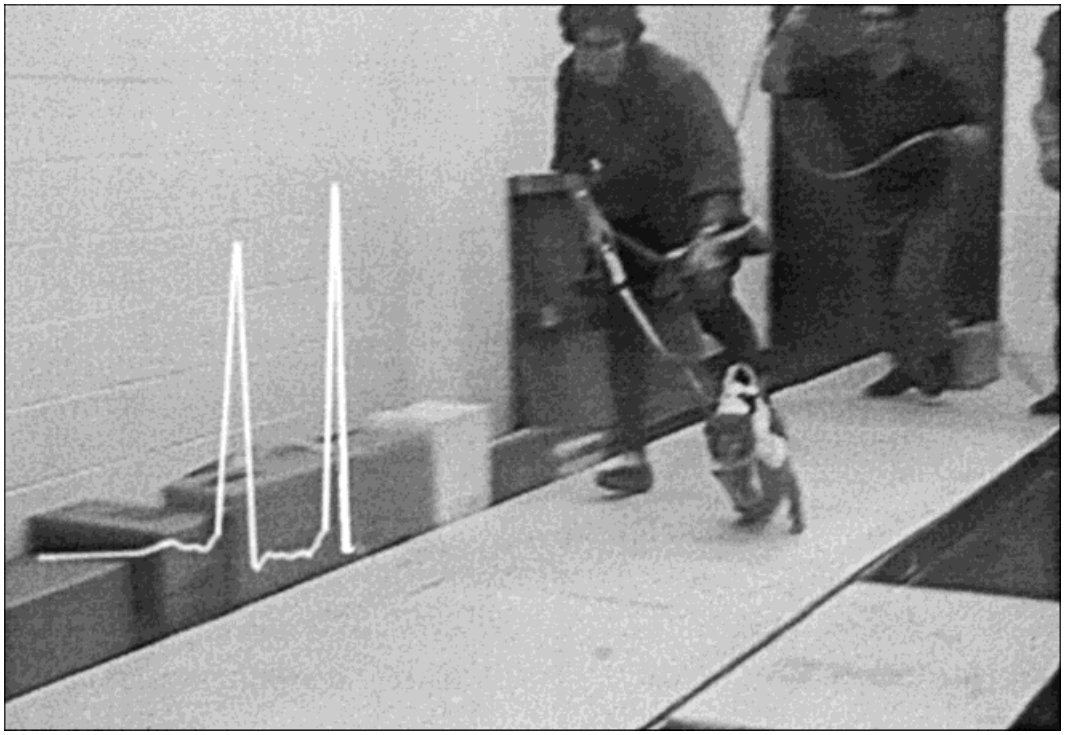

Fig. 1. Experimental setup. Strain gauges are attached to the ulna on the subject's left side. Wires run subcutaneously to the shoulder, where they surface and are attached to a connector carried in a pouch of a vest worn by the animal. The cable from the connector runs up a pole attached to the animal's neck collar and, from there, to the animal trainer and in a long loop to the computer. The superimposed trace is the reading from a single element of one of the rosette gauges, which was used to synchronize strain records and animal action. The image was taken from videotape.

posterolateral flange that contacts the ulnar olecranon in more extended joint positions and an anteromedial flange that has more extensive contact in flexed positions (Rose, 1988). The supposed function of mediolateral buttressing of the elbow joint remains hypothetical without knowledge of the forces acting in the frontal plane.

MATERIALS AND METHODS

Experiments were performed on three adult female rhesus macaques. Prior to surgery, the animals were trained to walk with a pole attached to a collar. Strain gauge implantation and data collection followed the protocol outlined in Gross et al. (1992). While the animal was under general anesthesia, a single incision approximately 6 cm long was made on the dorsoulnar aspect of the forearm. Three rectangular, three-element rosette gauges (Kenkyujo, Tokyo, Japan; 2 mm long) were placed around the circumference of the ulna at approximately one-third of its length from the distal end. Muscles and tendons were retracted, but no muscle attachments were interrupted. The gauge sites were exposed by scraping small areas of the cortical surface clean of periosteum. Subsequently, the surfaces were dried with 100% chloroform, and the gauges were glued on with isobutyl 2-cyanoacrylate monomer. To provide strain relief to the gauges, small expoxy resin flanges were screwed into the bone 2 cm proximal to the gauge sites, several times the distance at which local stress concentrations around the screw would affect strains measured by the gauges (Timoshenko, 1958; Gross et al., 1992). The wires from the gauges were run subcutaneously to the vicinity of the shoulder, where they exited through a small incision. There, they were soldered to a 25-pin connector.

Fig. 2. X-ray of the forearm of animal 3 showing the gauges and wires running up to the arm and shoulder. The three screws are holding resin flanges attached to the wires for strain relief.

The animals wore a vest to hold the connector in place and to prevent them from reaching it (Fig. 1).

In the first two experiments, data were collected with the Vishay Measurement Group (Raleigh, NC) 2110 amplifiers, and channels were sampled at 100 Hz; for the third experiment, Syminex Inc. (Marseille, France) model SX 500 amplifiers collected strains at 409.6 Hz. Individual sampling periods were 10 seconds long. The animals were videotaped during the trials. One strain channel was displayed on an oscilloscope. A video image of the oscilloscope was superimposed on that of the animal with a special-effects generator, thereby enabling synchronization of strain events and animal activity.

Qualitative comparisons were performed between gaits recorded preoperatively and postoperatively. Analyzed sequences were not observably different from those seen prior to the instrumentation of the ulna. Because the animals were allowed to move freely in any direction, video recordings were not obtained in standard planes required for quantitative gait analysis. The animals engaged in apparently normal locomotion shortly after recovery from anesthesia. No signs of lameness or favoring of limbs were apparent. Data were gathered at this time and again 2 days after surgery. Strains during walking, galloping, and climbing were recorded. After the second period of data collection, the animal was again anesthetized, and x-rays and computed tomography (CT) scans of the forearm were taken to document gauge positions. Prior to gauge removal, passive loading of the forearm of the anesthetized animal in axial compression, axial tension, and bending in four directions was performed to check proper gauge function and to verify gauge positions. All three gauges were found to be bonded firmly to the bone upon removal in two animals (animals 1 and 3). One of the three gauges was found loose in animal 2, and data from that gauge were discarded. Low strain readings had already raised the suspicion that this gauge was not functioning properly. Recovery was uneventful in each of the three animals.

Data were analyzed in a subroutine of the Macintosh program Igor (WaveMetrics, Inc. Lake Oswego, NY). By definition, principal strains are the greatest tensile (positive) and compressive (negative) strains in a planar strain field and are at right angles to one another. They were calculated for each rosette and for each sampling point over a locomotor cycle by using standard engineering equations (Dally and Riley, 1991). In addition, the angle of the maximum (tensile) principal strain relative to the long axis of the bone was calculated by using the orientation of the gauge relative to the long axis, as determined on the x-rays (Fig. 2). The exact

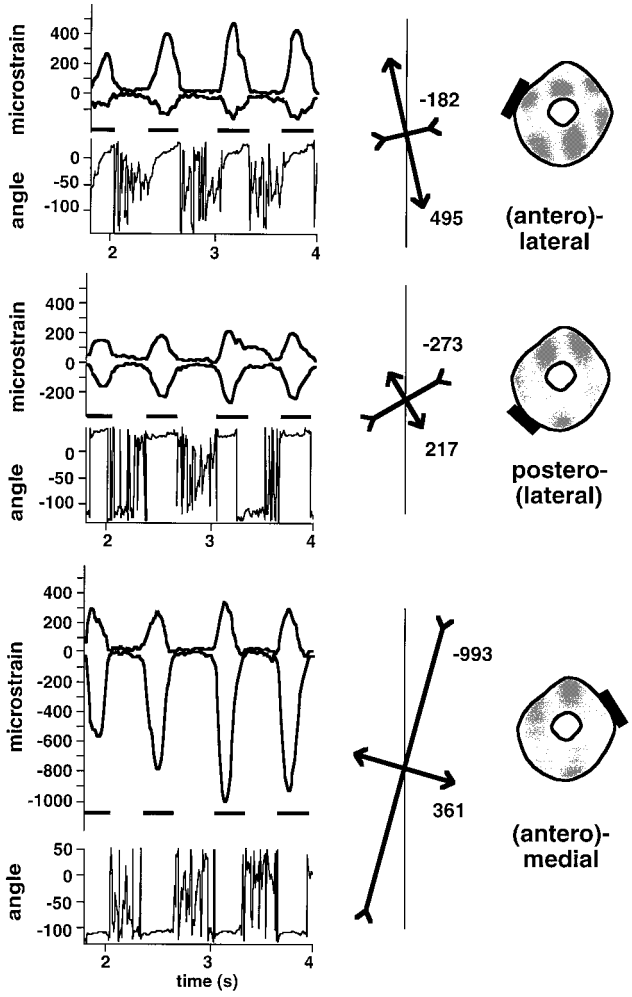

Fig. 3. Principal strain magnitudes and directions for three gauge sites of animal 1. The graphs on the left indicate the principal tensile (positive) and principal compressive (negative) strains as well as the angle of the principal tensile strain to the long axis of the bone for four consecutive walking steps. The horizontal bars indicate the support phases. The arrows are graphic representations of the mean peak principal tensile and compressive strains for each gauge location. Exact gauge locations are shown on the right.

positions of the gauges around the circumference of the bone were identified on the CT scans. Gauge sites were not exactly homologous in the three animals (see below). For each support phase, peak principal strains were identified, and means of the peak strains for all analyzed support phases were calculated for each gauge. For the two animals with strain readings from a complete set of three gauges, the distribution of normal (tensile and compressive) strains in the cross section of the ulna at the level of the gauge sites was calculated by using combined beam and finite element model analysis (see Rybicki et al. 1977; Gross et al., 1992; calculations courtesy T. Gross and Y.-X. Qin). This required knowledge of the cross-sectional geometry of the bone at the level of the gauge sites, which was determined from CT scans.

RESULTS

Peak principal strains in walking

Although an effort was made to place gauges on the medial, lateral, and posterior cortices of the ulna, in two animals, the actual positions deviated slightly from these gross anatomical directions. This is indicated in Figures 3–5. Nevertheless, we will refer to the gauge sites as medial, lateral, and posterior across animals. We report strains for walking steps for all three animals and for gallops for one of the animals.

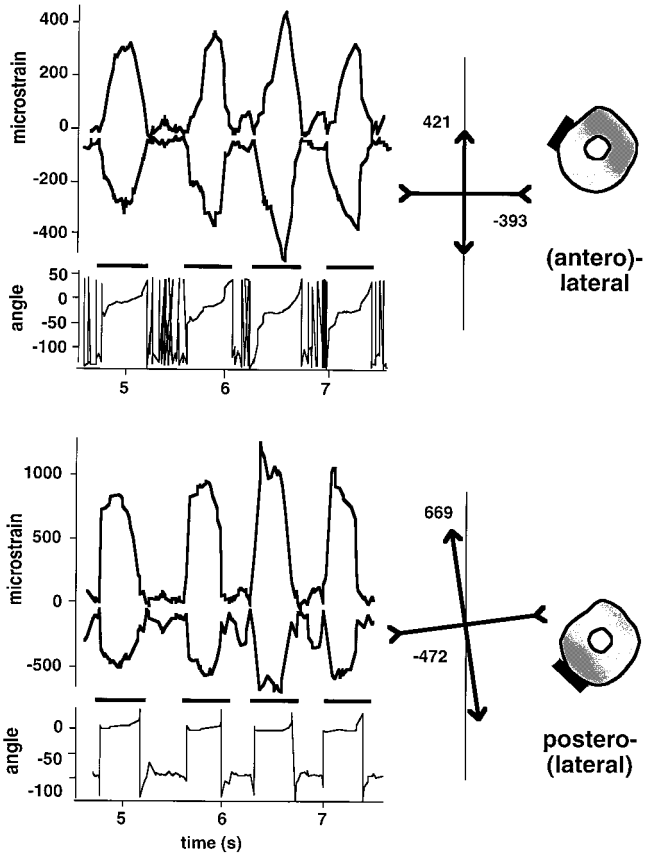

Fig. 4. Principal strain magnitudes and directions for two gauge sites of animal 2. For explanation, see Figure 3 legend.

Sampling frequencies of the amplifiers in the first two experiments were not high enough to capture strain dynamics adequately at the higher speed gait. Average values of peak principal strains and strain angles for all working gauges over all analyzed gait cycles are given in Table 1. Figures 3–5 illustrate strains over time for four consecutive steps of each animal. The mean magnitude and orientation of the peak principal strains relative to the long axis of the bone are also indicated.

Compressive strain predominates at the medial cortex (Table 1). Strain angles are very consistent within each animal but vary across the two animals for which data from this aspect of the bone are available. The principal compressive strain is aligned more closely with the long axis of the bone in these two animals. The strain on the medial cortex in the direction of the long axis of the ulna, therefore, is compressive (Figs. 3–5).

At the lateral cortex, principal tensile strain is higher than principal compressive strain (Table 1). Strain magnitudes vary considerably between animals. The strain angles also vary, with the principal tensile strain closely aligned with the long axis of the bone in animals 1 and 2 and deviating by almost 45° from the long axis in animal 3. Nonetheless, because the principal tensile strain is much higher than the principal compressive strain in animal 3, the strain in the direction of the long axis of the bone is tensile, as it is in animals 1 and 2.

The posterior cortex experiences principal strains that are more similar in magnitude to one another, with principal compression slightly higher in animals 1 and 3 and principal tension higher in animal 2. Equally variable is the alignment of the principal strains with the long axis of the bone. The longitudinal strain for this gauge site in

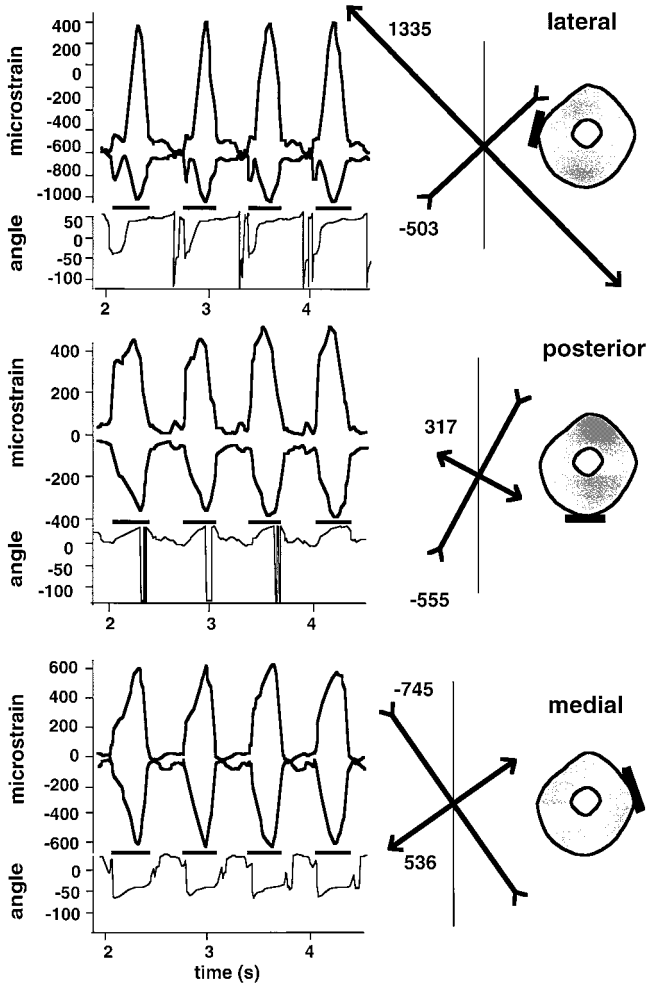

Fig. 5. Principal strain magnitudes and directions for three gauge sites of animal 3. For explanation, see Figure 3 legend.

animal 1 is very low and compressive, is higher and tensile in animal 2, and is of intermediate magnitude and compressive in animal 3 (Figs. 3–5, Table 1).

Normal strain distribution in walking

For animals 1 and 3, in which all rosette gauges were operative, normal strains calculated across a section through the ulna at the level of the gauge sites indicate a bending regime. The neutral axis ran from anteromedial to posterolateral throughout the stance phase in both animals (Figs. 6, 7). At the neutral axis of bending, normal strains go through zero and change from tension to compression. The direction of the neutral axis remained almost unchanged throughout the support phase, but the amount of bending changed, as indicated by the maximum strain magnitudes at the medial and lateral margins of the bone. Bending strains were highest around midsupport. In animal 2, the strains recorded from the two surfaces with functioning gauges are consistent with a bending regime similar to that of the other two animals.

Principal strains in galloping

Peak strain magnitudes and directions do not differ between walking and galloping steps for all three gauge sites in animal 3

TABLE 1. Peak principal strains and principal strain angles for the stance phase of locomotion[1]

	Lateral	Posterior	Medial
Walking steps			
Animal 1 (n = 17)[2]			
Max. principal strain	495 ± 67	217 ± 44	361 ± 128
Min. principal strain	−182 ± 28	−273 ± 31	−993 ± 150
Angle	12 ± 2	29 ± 3	73 ± 2
Animal 2 (n = 12)			
Max. principal strain	421 ± 100	669 ± 83	
Min. principal strain	−393 ± 133	−472 ± 175	
Angle	0 ± 4	8 ± 2	
Animal 3 (n = 18)			
Max. principal strain	1335 ± 318	317 ± 89	536 ± 84
Min. principal strain	−503 ± 128	−555 ± 197	−745 ± 267
Angle	41 ± 3	63 ± 16	126 ± 4
Gallops			
Animal 3 (n = 6)			
Max. principal strain	1099 ± 240	187 ± 47	346 ± 52
Min. principal strain	−385 ± 90	−555 ± 135	−588 ± 102
Angle	44 ± 1	66 ± 8	128 ± 2

[1] Strains are given in microstrain: Mean values ± 1 standard deviation. Angle of the maximum (Max.) principal strain with the longitudinal axis of the bone in counterclockwise direction. Min., minimum.
[2] For the medial gauge on the second day of recording, n = 11.

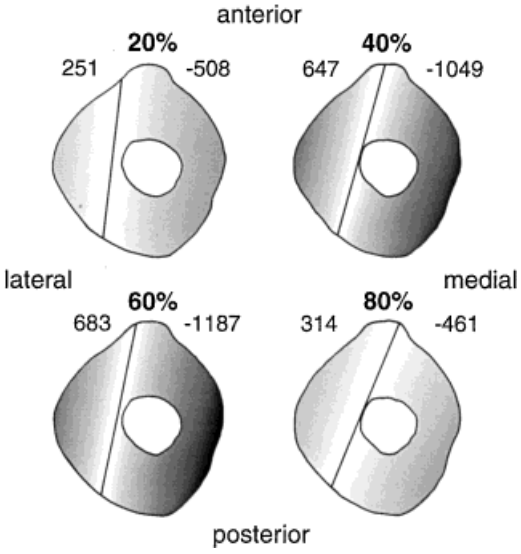

Fig. 6. Distribution of normal (tensile and compressive) strains in cross sections through the ulna of animal 1. Numbers indicate strains in the outer fibers of the bone, and lines represent the neutral axis of bending. Normal strains are shown at 20%, 40%, 60%, and 80% through the support phase.

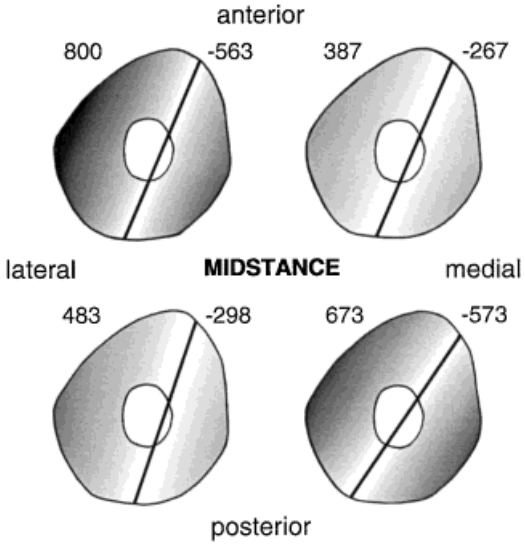

Fig. 7. Distribution of normal strains in the cross section of the ulna of animal 3. Peak strains for four stance phases are shown. Numbers indicate strains in the outer fibers of the bone, and lines represent the neutral axis of bending.

(Table 1). Figure 8 illustrates the principal strains and strain angles for a sequence of steps that includes a change in gait from walking to galloping. The transitional step is characterized by a slight drop in strain magnitudes, but, otherwise, strain patterns are unchanged.

DISCUSSION

The data suggest that one loading regime—mediolateral bending—is present in the ulna of all three animals. Although there are subtle differences in strain magnitudes and directions, in essence, the longitudinal strain on the lateral cortex is tensile, and the longitudinal strain on the medial cortex

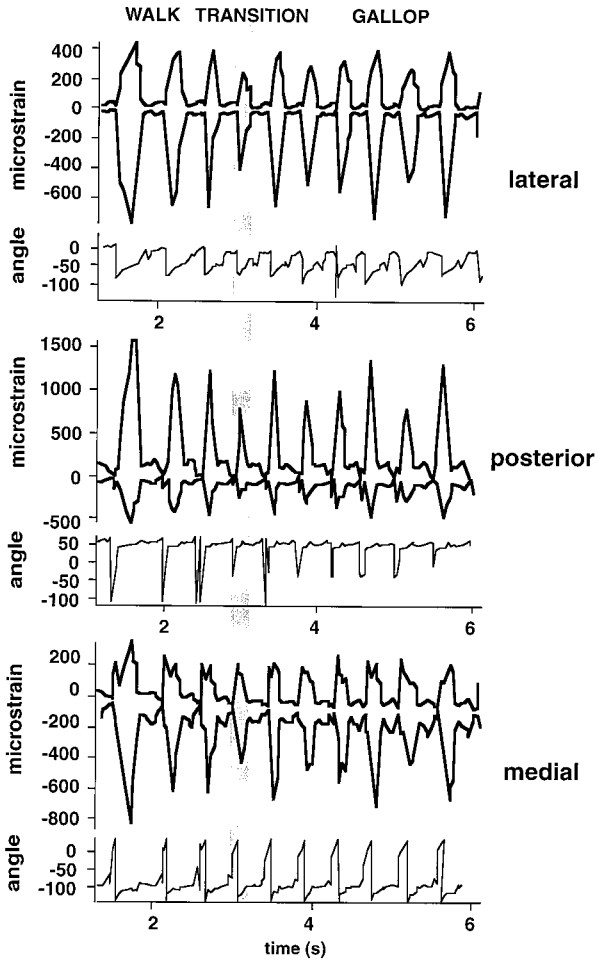

Fig. 8. Principal strain magnitudes and angles of the principal tensile strain with the long axis of the ulna for a sequence of steps of animal 3 that includes a gait transition from walk to gallop.

is compressive. The posterior cortex shows some variability in magnitude and direction, much of which can be attributed to small differences in the gauge attachment sites. More specifically, as illustrated in Figures 3–5, the "posterior" gauges in animals 1 and 2 are posterolateral gauges, and, with the neutral axis of bending inclined from anteromedial to posterolateral, these gauges would fall into tension or read low strains, depending on their precise position relative to the neutral axis of bending. For animal 3, the posterior gauge would lie on the compressive side of such a neutral axis.

Mediolateral bending is not the loading regime that we had predicted for the rhesus monkey ulna. Other in vivo studies of long bone strain report anteroposterior bending (sheep radius: Lanyon and Baggott, 1976; radius and tibia of horse and dog: Rubin and Lanyon, 1982; horse radius: Biewener et al., 1983; goat tibia and radius: Biewener and Taylor, 1986; horse tibia: Biewener et al., 1988), and this was our anticipation in the current study. On the other hand, Gross et al. (1992) report tension not only for the anterior cortex but also for a small part of the lateral cortex of the horse metacarpal, and Biewener and Bertram (1993) measured compression on the cranial (anterior) and medial cortices of the chicken tibiotarsus, a pattern similar to our findings.

To determine an explanation for our findings, we examined kinematic and kinetic data collected on the same macaques. We observed that the animals closely align their

Fig. 9. Frontal view of animal 3 with the left (instrumented) forelimb at midstance of a walking step. Note the position of the elbow lateral to the substrate contact. The superimposed force vector indicates the average inclination of the ground reaction force in the frontal plane in walking macaques (courtesy of D. Schmitt).

forearms with the substrate reaction force vector in the sagittal plane, especially around midstance, when the reaction forces are highest (Schmitt, 1995). Anteroposterior bending moments, therefore, may be minor. Macaques walk with their elbows positioned lateral to the point of substrate contact (Fig. 9). The substrate reaction force vector is inclined medially by an angle of around 5° (Schmitt, in preparation). Thus, it will pass medial to the forearm and produce medially concave bending of the ulna (Fig. 9). Greater frontal plane than sagittal plane substrate reaction moments were also reported for the leg and knee of humans during the stance phase of walking (Schipplein and Andriacchi, 1991).

If mediolateral bending of the ulna is indeed caused by the ground reaction force vector passing on the medial side of the bone, then it is strongly suggested that this force exerts an adducting torque at the elbow joint. This can be counteracted by the lateral flange of the trochlea that contacts the ulna in joint positions close to extension (Rose, 1988). The effect of the radius on ulnar loading is difficult to assess. Because the forearm is pronated, part of the radius is positioned not only to the medial and lateral sides of the ulna but also crosses it anteriorly; therefore, it may contribute to the strength of the forearm in frontal and sagittal planes. Our data cannot reveal the complete loading regime of the forearm but only that of the ulna in an intact forearm.

The shaft diameters of the macaque ulna do not reveal any obvious mediolateral reinforcements to counteract mediolateral bending moments. On the contrary, the anteroposterior diameter exceeds the mediolateral diameter. The x-rays as well as the CT scans taken from our experimental animals do not indicate that the cortex of the shaft is thickened on the medial and lateral sides. Conventional interpretations of long bone geometry are based on the assumption that bones are reinforced in the loaded plane (see, e.g., Pauwels, 1950, 1954; Trinkaus and Ruff, 1989; Ruff and Runestad, 1992; Demes and Jungers, 1993; however, for an alternate view, see Lanyon and Rubin, 1985). Our results confirm recent evidence that minimization of bone tissue may not be the primary goal of bone adaptation (Rubin et al., 1990, 1994). Bone cross-sectional geometry may not be a simple mirror reflection of functional loads.

The deviations of principal strains from the long axis of the ulna indicate that the observed strains are not the result of only axial loading and bending. A superimposed torsional regime is the likely source of the off-axis strain components. This torsional moment could result from rotation that is resisted at the humero ulnar joint. It is unclear what causes the variation between animals. There were no obvious differences in forelimb movements between them.

The peak strain magnitudes we measured are well below the 2,000–3,000 με range often reported for other animals during strenuous activity (Rubin and Lanyon, 1982,

TABLE 2. Comparison of average peak principal strain magnitudes for the stance phase of walking

Species	Bone	Cortex	Activity	Greatest principal strain[1]	Source
Sheep	Tibia	Cranial	Walk	709	Lanyon and Bourn, 1979
		Caudal	Walk	−666	
Sheep	Radius	Cranial	Walk	688	Lanyon et al., 1979
		Caudal	Walk	−1161	
Sheep	Radius	Cranial	Walk	807	Lanyon and Baggott, 1976
		Caudal	Walk	−1317	
Goat	Tibia	Caudal	Slow walk	−725	Biewener and Taylor, 1986
		Caudal	Fast walk	−845	
	Radius	Caudal	Slow walk	−822	
		Caudal	Fast walk	−832	
Dog	Tibia	Caudal	Slow walk	−702	Rubin and Lanyon, 1982
		Caudal	Fast walk	−1059	
Dog	Radius	Caudal	Walk	−1503	
Horse	Tibia	Caudal	Slow walk	−939	
		Caudal	Fast walk	−1347	
	Radius	Caudal	Slow walk	−1777	
		Caudal	Fast walk	−1965	
Horse	Tibia	Caudal	Fast walk	−998	Biewener and Taylor, 1986
	Radius	Caudal	Fast walk	−1247	
Human	Tibia	Medial	Walk	−544	Burr et al., 1996
Human	Tibia	Medial	Walk	−400	Lanyon et al., 1975
Macaque	Ulna	Medial	Walk	−869	Present study; mean values for all animals
		Lateral	Walk	915	
		Posterior	Walk	433	

[1] Strains are given in microstrains and represent mean values for several step cycles that, in most cases, cover a range of speeds.

1984). Indeed, this latter level of strain has been proposed to be beneficial for bone tissue and to be maintained through kinematic adjustments (speed, joint angles) over wide ranges of body sizes and locomotor modes ("dynamic strain similarity": Rubin and Lanyon, 1984; Rubin et al., 1994; "stress similarity": Biewener, 1989). Even if peak strain levels are compared for walking gaits only, the measured strains in the macaque ulna are still relatively low, but they do overlap with strains measured in the human tibia, sheep and goat tibiae and radii, and dog and horse tibiae (Table 2). Low strain magnitudes could be a result of low ground reaction forces. However, primate quadrupeds, including macaques, are not characterized by lower reaction forces acting on their forelimbs during walking on the ground than nonprimate quadrupeds (Fig. 10). Primate long bones also do not possess greater rigidity in static bending (Polk et al., 1997). An alternative explanation for the rather low strains in the ulna is that the radius transmits a greater share of the loads acting on the forearm.

Contrary to other studies that have documented strain gradients at gait transitions and an increase in strain magnitudes with speed for horses, dogs, and goats (Rubin and Lanyon, 1982; Biewener et al., 1983, 1988; Biewener and Taylor, 1986), we found that strain magnitudes were similar for walks and gallops and found no incremental change at gait transition. The change from trot to gallop in nonprimate mammals is usually accompanied by a decrease in strains, wherease the walk-to-trot transition is characterized by an increase. Primates do not use the high-cadence, high-force trot but change from walking directly into a gallop (Hildebrand, 1967; Vilensky, 1983; Preuschoft et al., 1996). Strains in nonprimate mammals galloping at slow speeds are considerably higher than strains at fast walks (Rubin and Lanyon, 1982; Biewener and Taylor, 1986). This suggests that at least the slow gallop in primates may be more compliant than the gallop of nonprimate mammals (cf. Schmitt, 1995). This is confirmed by ground reaction forces that do not change much at gait transition in primates (Demes et al., 1994).

CONCLUSIONS

Bone strain in the macaque ulna indicates mediolateral bending as the predominant loading regime during the stance phase of walking. The bending moment is probably

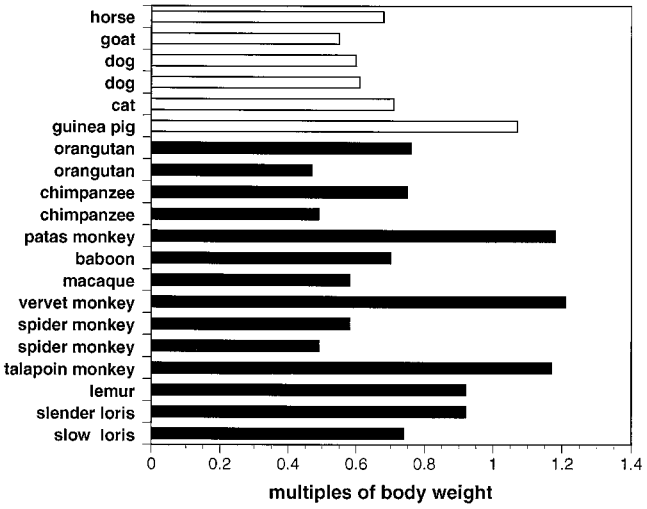

Fig. 10. Comparison of walking ground reaction force magnitudes for the forelimbs of primate and nonprimate quadrupeds. Peak stance phase forces are indicated in multiples of body weights; in most cases, they represent means for forces recorded for a range of speeds not specifically stated in the references (Budsberg et al., 1987; Demes et al., 1994; Ishida et al., 1990; Kimura, 1985; Nieschalk, 1991; Pandy et al., 1988; Reynolds, 1985; Roush and McLaughlin, 1994; Ueda et al., 1981; Biknevicius, personal communication).

caused by the ground reaction force vector that passes medial to the forearm. The macaque ulna is not reinforced in the plane of bending. The lack of buttressing in the loaded plane and the somewhat counterintuitive bending direction recommend caution with regard to conventional interpretations of long bone cross-sectional geometry. Gait change from walk to gallop is not accompanied by an incremental change in strain magnitudes. This result mirrors the absence of a significant change in ground reaction forces at the walk-gallop transition of primates.

ACKNOWLEDGMENTS

Ted Gross and Yi-Xian Qin provided the calculations of normal strain distributions in the cross sections of the ulnae. Ted Gross and Susannah and Chris Fritton helped in data collection and analysis. David Reim assisted in the surgery. Terry Button took the CT scans and x-rays in the middle of the night. Xinbin Chen wrote part of the programs used for data analysis. We thank all of them for their invaluable contributions to this project.

LITERATURE CITED

Alexander RMN, Hayes AS, Maloiy GMO, and Wathuta EM (1979) Allometry of the limb bones of mammals from shrews (*Sorex*) to elephant (*Loxodonta*). J. Zool. Lond. *189:*305–314.

Alexander RMN, and Maloiy GMO (1984) Stride lengths and stride frequencies of primates. J. Zool. London *202:*577–582.

Biewener AA (1989) Scaling body support in mammals: Limb posture and muscle mechanics. Science *245:* 45–48.

Biewener AA, and Bertram JEA (1993) Skeletal strain patterns in relation to exercise training during growth. J. Exp. Biol. *185:*51–69.

Biewener AA, and Taylor CR (1986) Bone strain: A determinant of gait and speed? J. Exp. Biol. *123:*383–400.

Biewener AA, Thomason J, Goodship A, and Lanyon LE (1983) Bone stress in the horse forelimb during locomotion at different gaits: A comparison of two experimental methods. J. Biomech. *16:*565–576.

Biewener AA, Thomason JJ, and Lanyon LE (1988) Mechanics of locomotion and jumping in the horse (Equus): In vivo stress in the tibia and metatarsus. J. Zool. London *214:*547–565.

Bouvier M, and Hylander WL (1984) In vivo bone strain on the dog tibia during locomotion. Acta Anat. *118:*187–192.

Budsberg SC, Verstraete MC, and Soutas-Little RW (1987) Force plate analysis of the walking gait in healthy dogs. Am. J. Vet. Res. *48:*915–918.

Burr DB, Milgrom C, Fyhrie D, Forwood M, Nysaka M, Finestone A, Hoshaw S, Saiag E, and Simkin A (1996) In vivo measurement of human tibial bone strain during vigorous activity. Bone *18:*405–410.

Carter DR, Vasu R, Spengler DM, and Dueland RT (1981) Stress fields in the unplated and plated canine femur calculated from in vivo strain measurements. J. Biomech. *14:*63–70.

Dally JW, and Riley WF (1991) Experimental Stress Analysis, 3rd ed. New York: McGraw-Hill.

Demes B, and Jungers WL (1993) Long bone cross-sectional dimensions, locomotor adaptations and body size in prosimian primates. J. Hum. Evol. *25:*57–74.

Demes B, Larson SG, Stern JT Jr, Jungers WL, Biknevicius AR, and Schmitt D (1994) The kinetics of primate quadrupedalism: "Hindlimb drive" reconsidered. J. Hum. Evol. *26:*353–374.

Fleagle JG (1983) Locomotor adaptations of Oligocene and Miocene hominoids and their phyletic implications. In Ciochon RL and RS Corruccini (eds.): New Interpretations of Ape and Human Ancestry. New York: Plenum Press, pp. 301–324.

Fleagle JG, Simons EL, and Conroy GC (1975) Ape limb bone from the Oligocene of Egypt. Science *189:*135–137.

Fleagle JG, Stern JT Jr, Jungers WL, Susman RL, Vangor AK, and Wells JP (1981) Climbing: A biomechanical link with brachiation and with bipedalism. Symp. Zool. Soc. London *48:*359–375.

Goodship AE, Lanyon LE, and MacFie H (1979) Functional adaptation of bone to increased stress. J. Bone Joint Surg. *61A:*539–546.

Gross TS, McLeod KJ, and Rubin CT (1992) Characterizing bone strain distributions in vivo using three triple rosette strain gauges. J. Biomech. *25:*1081–1087.

Harrison T (1989) New postcranial remains of *Victoria pithecus* from the middle Miocene of Kenya. J. Hum. Evol. *18:*3–54.

Hildebrand M (1967) Symmetrical gaits of primates. Am. J. Phys. Anthropol. *26:*119–130.

Ishida H, Jouffroy, FK, and Nakano Y (1990) Comparative dynamics of pronograde and upsidedown horizontal quadrupedalism in the slow loris (*Nycticebus coucang*). In Jouffroy FK, MH Stack, and C Niemitz (eds.): Gravity, Posture and Locomotion in Primates. Firence: Il Sedicesimo, pp. 209–220.

Jenkins FA Jr (1973) The functional anatomy and evolution of the mammalian humero-ulnar articulation. Am. J. Anat. *137:*281–298.

Kimura T (1985) Bipedal and quadrupedal walking of primates: Comparative dynamics. In Kondo S (ed.): Primate Morphophysiology, Locomotor Analyses and Human Bipedalism. Tokyo: University of Tokyo Press, pp. 81–104.

Kimura T (1995) Long bone characteristics of primates. Z. Morphol. Anthropol. *80:*265–280.

Kimura T, Okada M, and Ishida H (1979) Kinesiological characteristics of primate walking: Its significance in human walking. In Morbeck ME, H Preuschoft, and N Gomberg (eds.): Environment, Behavior and Morphology: Dynamic Interactions in Primates. New York: G. Fischer, pp. 297–311.

Lanyon LE, and Baggott DG (1976) Mechanical function as an influence on the structure and form of bone. J. Bone Joint Surg. *58B:*436–443.

Lanyon LE, and Bourn S (1979) The influence of mechanical function on the development and remodelling of the tibia. An experimental study in sheep. J. Bone Joint Surg. *61A:*263–273.

Laynon LE, and Rubin CT (1985) Functional adaptation in skeletal structures. In Hildebrand M, DM Bramble, KF Liem, and DB Wake (eds.): Functional Vertebrate Morphology. Cambridge: Harvard University Press, pp. 1–25.

Lanyon LE, and Smith RN (1969) Measurement of bone strain in the walking animal. Res. Vet. Sci. *10:*93–94.

Lanyon LE, and Smith RN (1970) Bone strain in the tibia during normal quadrupedal locomotion. Acta Orthop. Scand. *41:*238–248.

Lanyon LE, Hampson WGJ, Goodship AE, and Shah JS (1975) Bone deformation recorded in vivo from strain gauges attached to the human tibial shaft. Acta Orthop. Scand. *46:*256–268.

Lanyon LE, Magee PT, and Baggott DG (1979) The relationship of functional stress and strain to the processes of bone remodelling. An experimental study on the sheep radius. J. Biomech. *12:*593–600.

Nieschalk U (1991) Fortbewegung und Funktionsmorphologie von *Loris tardigradus* und anderen kleinen quadrupeden Halbaffen in Anpassung an unterschiedliche Habitate [Ph.D. thesis]. Ruhr-Universität Bochum.

Pandy MG, Kumar V, Berme N, and Waldron KJ (1988) The dynamics of quadrupedal locomotion. J. Biomech. Eng. *110:*230–237.

Pauwels F (1950) Die Bedeutung der Muskelkräfte für die Regelung der Beanspruchung des Röhrenknochens während der Bewegung der Glieder. Z. Anat. Entwickl. Gesch. *115:*326–351.

Pauwels F (1954) Die statische Bedeutung der *Linea aspera*. Z. Anat. Entwickl. Gesch. *117:*497–503.

Polk JD, Demes B, Jungers WL, Heinrich RE, Biknevicius AR, and Runestad JA (1997) Cross-sectional properties of primate and nonprimate limb bones. Am. J. Phys. Anthropol. *24(Suppl.):*188.

Preuschoft H, Witte H, Christian A, and Fischer M (1996) Size influences on primate locomotion and body shape, with special emphasis on the locomotion of 'small mammals'. Folia Primatol. *66:*93–112.

Reynolds TR (1985) Stresses on the limbs of quadrupedal primates. Am. J. Phys. Anthropol. *67:*351–362.

Reynolds TR (1987) Stride length and its determinants in humans, early hominids, primates, and mammals. Am. J. Phys. Anthropol. *72:*101–115.

Richmond BG, Fleagle JG, Kappelman J, and Swisher CC (1998) First hominoid from the Miocene of Ethiopia and the evolution of the catarrhine elbow. Am. J. Phys. Anthropol. (in press).

Rose MD (1988) Another look at the anthropoid elbow. J. Hum. Evol. *17:*193–224.

Roush JK, and McLaughlin RM (1994) Effects of subject stance time and velocity on ground reaction forces in clinically normal Greyhounds at the walk. Am. J. Vet. Res. *55:*1672–1676.

Rubin CT, and Lanyon LE (1982) Limb mechanics as a function of speed and gait. J. Exp. Biol. *101:*187–211.

Rubin CT, and Lanyon LE (1984) Dynamic strain similarity in vertebrates: An alternative to allometric limb bone scaling. J. Theor. Biol. *107:*321–327.

Rubin CT, McLeod KJ, and Bain SD (1990) Functional strains and cortical bone adaptation: Epigenetic assurance of skeletal integrity. J. Biomech. *23(Suppl. 1):* 43–54.

Rubin C, Gross T, Donahue H, Guilak F, and McLeod K (1994) Physical and environmental influences on bone formation. In: Brighton CT, GE Friedlaender, and JM Lane (eds.): Bone Formation and Repair. Rosemont: American Academy of Orthopedic Surgeons, pp. 61–78.

Ruff CB, and Runestad JA (1992) Primate limb bone structural adaptations. Annu. Rev. Anthropol. *21:*407–433.

Rybicki EF, Mills EJ, Turner AS, and Simonen FA (1977): In vivo and analytical studies of forces and moments in equine long bones. J. Biomech. *10:*701–795.

Schipplein OD, and Andriacchi TP (1991) Interactions between active and passive knee stabilizers during level walking. J. Orthop. Res. *9:*113-119.

Schmitt D (1994) Forelimb mechanics as a function of substrate type during quadrupedalism in two anthropoid primates. J. Hum. Evol. *26:*441–457.

Schmitt D (1995) A Kinematic and Kinetic Analysis of Forelimb Use During Arboreal and Terrestrial Quadrupedalism in Old World Monkeys [PhD thesis]. State University of New York at Stony Brook.

Swartz SM, Bertram JEA, and Biewener AA (1989) Telemetered in vivo strain analysis of locomotor mechanics of brachiating gibbons. Nature *342:*270–272.

Swartz SM, Bennett MB, and Carrier DR (1992) Wing bone stresses in free flying bats and the evolution of skeletal design for flight. Nature *359:*726–729.

Timoshenko S (1958) Strength of Materials. Part II, 3rd ed. New York: D. van Norstand Co.

Trinkaus E, and Ruff C (1989) Diaphyseal cross-sectional morphology and biomechanics of the Fond-de-Forêt 1 femur and the Spy 2 femur and tibia. Anthropologie Préhistoire *100:*33–42.

Ueda Y, Niki Y, Yoshida K, and Masumitsu H (1981) Force plate study of equine biomechanics—Floor reaction force of normal walking and trotting horses. Bull. Equine Res. Inst. *18:*28–41.

Vilensky JA (1983) Gait characteristics of two macaques, with emphasis on relationships with speed. Am. J. Phys. Anthropol. *61:*255–265.